Improvement of the homogeneity of magnetic field by the attenuation of a selected component with an open superconducting shield made of commercial tapes

Łukasz Tomków,[1,2,a)] Evgeniy Kulikov,[2] Kamil Kozłowski,[3] and Valeriy Drobin[2]

[1)] *Wroclaw University of Technology, Faculty of Mechanical and Power Engineering,*
Wybrzeże Wyspiańskiego 27, 50-370 Wrocław, Poland
[2)] *Joint Institute for Nuclear Research, Veksler and Baldin Laboratory of High Energy Physics,*
Joliot-Curie 6, 141980 Dubna, Moscow region, Russia
[3)] *GSI Helmholtz Centre for Heavy Ion Research,*
Planckstraße 1, 64291 Darmstadt, Germany

(Dated: 3 August 2019)

Homogeneous magnetic fields are needed in many applications. The resolution of medical imaging techniques depends on the quality of the magnetic field, so does the efficiency of electron cooling systems used at particle accelerators. Current methods of improving homogeneity require complex arrangements of magnet windings. In this work the application of commercial superconducting tapes for this purpose is analyzed experimentally and numerically. Shielding effect exhibited by the superconductors can be used to control the shape of magnetic field. An open magnetic shield made of superconducting tapes is able to nullify the radial component of a solenoidal magnetic field, forming the long region of the homogeneous magnetic field.

To form a shield the superconducting tapes are wound on a former. Then it is positioned coaxially inside an electromagnet. The measurements are performed in DC magnetic field and at zero-field cooling conditions. Numerical model is developed to further analyze the magnetic field. New simplifications and proper constraints allow the use of an axial symmetry despite relatively complex geometry of the shields. Results from the simplified model and obtained experimentally are consistent. The decrease of radial component of the magnetic field and the significant improvement of its homogeneity are observed in a shielded region. The decrease of shielding quality with the increase of an applied magnetic field is observed. Empirical formulas describing dependence of shielding quality on the geometry and the critical current of the shield are developed.

I. INTRODUCTION

Homogeneity of magnetic field is a desirable quality in multiple applications[1]. It can be improved using superconducting tapes made of high temperature superconductors (HTS)[2]. Currently used methods include shimming[3], active shields[4] and proper coil configurations[5]. The application of HTS shields is appealing as it is simple and efficient. Application of low temperature superconductors (LTS) for similar purpose was also proposed, such as the first application of a hollow superconducting cylinder for homogenization of the magnetic field[6]. LTS shields, however, have to be cooled with liquid helium and are viable option only if the supply of the cryogen is already present[7].

Most of the previous work on magnetic shielding with HTS focused on attenuation of the magnetic field. Bulk superconductors are capable of full shielding below a penetration magnetic field[8]. Hogan et al. analyzed the behavior of bulks in an inhomogeneous fringe magnetic field[9]. Notably, no homogenization of magnetic field was observed. Instead, the magnetic field was observed to concentrate in non-intuitive locations in the case of inhomogeneous fields or on the external surface of the sample if the applied field was symmetrical. Wéra et al. observed significant reduction of magnetic flux shielded by superconducting bulks even when the applied magnetic flux exceeded 1.5 T[10]. They also analyzed the effect of cap on the attenuation strength[11]. Fast numerical modelling methods were proposed for closed shields and magnetic lenses[12].

Magnetic shielding properties of the superconducting tapes were tested mostly in AC magnetic field. In this regime the magnetic field is decreased by the currents induced in the tapes[13]. The experiments and simulations were performed in the range of frequencies between 10 Hz and 144 Hz[14,15]. Some measurements in lower frequencies were also done[16]. Kvitkovic et al[17] and Wéra et al.[18,19] analyzed the geometrical effects on the shielding quality. Kvitkovic et al. also described the application of a planar magnetic shield to decrease the noise in the measurements of the magnetic field[20]. Magnetic shields made of superconducting tapes were applied to increase the operating magnetic field of superconductive integrated circuits[21] and the efficiency of contactless power transfer[22].

Using the shielding effect of the superconductors it is possible to create a magnetic cloak[23]. Such device is able to hide the magnetic effect of a surrounded object so that its presence does not change the magnetic field outside of the cloak. Application of a magnetic cloak was recently proposed to stop the interference between the particle beams[24]. To operate it requires the application of a superconducting insert acting as a magnetic shield. Both

a)Electronic mail: lukasz.tomkow@pwr.edu.pl

bulk and tape superconductors can be used[25].

Understanding shielding effects is important in the design of superconducting coils. It is expected to affect the stability of toroidal field coils of fusion reactor such as CFETR[26]. Application of a superconducting shield was observed to decrease the rate of the direct current decay in the coil subjected to an external AC field[27]. Superconducting RF cavities also require magnetic shielding, however the application of superconducting magnetic shields for this purpose has yet to be investigated[28].

The goal of this paper is to analyze the behavior of multilayer magnetic shields made of HTS tapes in terms of their usefulness to improve homogeneity of the magnetic field. A configuration in which a shield is placed coaxially inside a solenoidal electromagnet is considered. The shields are analyzed in the context of application at the electron cooling system of ion source KRION for particle accelerator NICA, currently under construction at Joint Institute for Nuclear Research in Dubna. Long region (in the range of few meters) of homogeneous magnetic field is required to obtain the high efficiency of the electron cooling process. Initial experimental studies of the system were performed[29].

The numerical analysis of the operation of the shield is performed. Previous works on similar applications focused on analytical considerations[2,30,31]. The results of numerical analysis allow better understanding of the behavior of the shield and ways to improve its efficiency. Axial symmetry is applied in the model and certain simplifications are applied. Despite them a good agreement between simulation and experiment is obtained. The results encourage to use the described procedure to estimate the shielding efficiency of any proposed design if the proper material data are available. The reaction of the shield to any configuration of an external magnetic field can be predicted using the proposed model.

II. METHODS

A. Model

The major difference between a closed and an open superconducting magnetic shield is the way the shielding electric currents are allowed to flow. In the closed shields the current flows freely in the volume of the superconductor. Such situation occurs when the superconductor is solid or if the tapes are somehow connected with lossless joints. If a coaxial configuration with a solenoidal magnetic field is considered, a closed shield would attenuate both components of the magnetic field with the shielding current J_ϕ flowing in opposite angular direction to that in the electromagnet, as shown in figure 1a. Such behavior leads to the complete disappearance of the magnetic field in a shielded cavity by the superposition of two solenoidal field patterns[8].

In an open shield the currents are restricted by the geometry of a tape and cannot flow around the axis of the assembly, as shown in figure 1b. In this case the current loops are formed to shield the interior of the superconducting material. It leads to the attenuation of the component of the field perpendicular to the surface of the shield. In the considered axial arrangement the component perpendicular to the surface of the tape corresponds with the radial component of the solenoidal field, leading to its attenuation. The component parallel to the surface of the tape is equalized behind it, therefore the axial component is homogenized.

Electric current density and the magnetic field distribution are found with a numerical model. The model was applied in Comsol using H-formulation, described further in this section[32]. The geometry of the shield is quite complex to recreate in the model. The shield consists of several layers of superconducting tapes that are not necessarily periodic with respect to each other. To avoid the need to use a 3D model some assumptions are made to allow the use of axial symmetry and modeling in 2D.

It is assumed that the currents flowing in the direction parallel to the axis compensate between neighboring tapes (currents J_z in figure 1b). Compensation is possible thanks = to the anisotropy of the critical current density in the tape. The width of the region in which J_z is carried is much smaller than J_{phi}. The currents flowing in r direction are neglected. According to these assumptions the magnetic field is affected only by current J_ϕ. In this case only radial component H_r and axial component H_z of the magnetic field $\mathbf{H}$ exist. To further decrease the computation time the symmetry of the system along z axis is exploited and only a half of the assembly is modeled.

The basic formula used in H-formulation is the combination of Ampère's law and Faraday's law (formula 1)[33]. It is assumed that the relative magnetic permeability of all regions is equal to 1, therefore it is neglected in the formulas.

$$\frac{\partial H_r}{\partial t} + \frac{\partial H_z}{\partial t} + \frac{1}{r}\frac{\partial}{\partial r}\left(r E_\phi(J_\phi)\right) - \frac{\partial}{\partial z}(E_\phi(J_\phi)) = 0 \quad (1)$$

Angular component of the electric field E_ϕ in the superconducting region (cross-section of the tape) is found with formula 2 employing the power law.

$$E_\phi = \begin{cases} E_0 \left(\frac{|J_\phi|-J_c}{J_c}\right)^n \frac{J_\phi}{|J_\phi|} & \text{when } |J_\phi| \geq J_c \\ 0 & \text{when } |J_\phi| < J_c \end{cases} \quad (2)$$

Exponent of power law n was assumed as 31 and the limit of the electric field E_0 as 100 $\mu V/m$[20]. J_ϕ is calculated as the rotation of the magnetic field with formula 3.

$$J_\phi = \frac{\partial H_r}{\partial z} - \frac{\partial H_z}{\partial r} \quad (3)$$

Calculation of critical current J_c is based on the experimental data obtained by Zhang et al.[34]. The dependence of the critical current on the orientation and strength of magnetic flux B is performed according to a procedure described by Zhang et al.[35] and described with formula
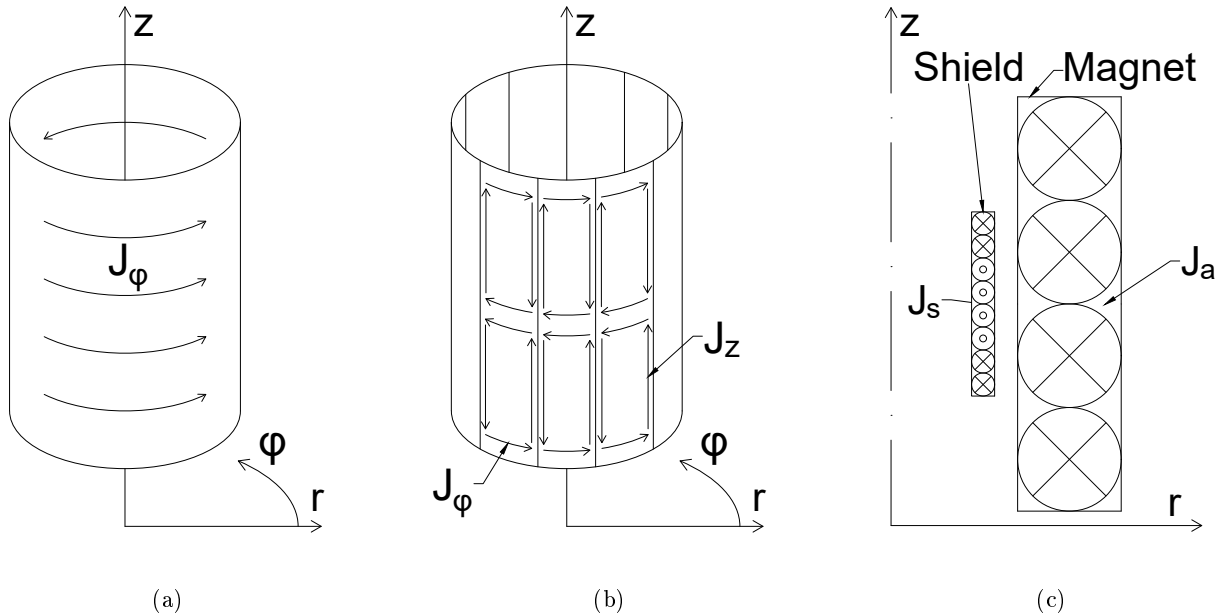
FIG. 1: Expected patterns of shielding currents and simplifying assumptions applied in the numerical model.
(a) Closed shield, (b) Open shield, (c) Simplified system

4. Values of J_{c0} and B_0 are material constants fitted to experimental data to reflect the behavior of the tape. Parameters of α, β and γ^2 are based on those for SCS6050 tape and are 1, 0.67 and 7.69 respectively. B is calculated as $\sqrt{(\mu_0 H_r)^2 + (\mu_0 H_z)^2}$, ϵ is calculated with formula 5.

$$J_c = J_{c0} \left[1 + \epsilon \frac{B}{B_0}^{\alpha} \right]^{-\beta} \qquad (4)$$

$$\epsilon = \sqrt{\gamma^{-2} \cdot \left(\frac{B_z}{B}\right)^2 + \left(\frac{B_r}{B}\right)^2} \qquad (5)$$

The actual thickness of the shield domain in the model is significantly larger (by the factor of 100) than that of superconducting layer and is close to the thickness of entire tape (approximately 100 μm). Such approach reduces the number of required nodes and improves the stability of the model. To account for that change the value of critical current is adjusted. The total current carrying-capacity of the domain is the same as combined critical current of all layers of tapes forming the shield.
In the normal region E_ϕ is found with formula 6. ρ is the resistivity of a material.

$$E_\phi = \rho \cdot J_\phi \qquad (6)$$

The simplified model and the expected pattern of electric currents is presented in figure 1c. The thickness of the shield is exaggerated. On the external boundaries of the model region the condition of magnetic insulation is imposed, forcing the magnetic field to be parallel to the boundary. To account for the symmetry of the system the condition of perfect magnetic conductor is applied on the boundary dividing the magnetic shield in half, forcing the lines of magnetic field to be perpendicular to the boundary. Operation of an electromagnet is simulated by the region of uniform current density J_a in direction ϕ. Its value is adjusted to match the strength of the field generated by the electromagnets used during the experiments. Axial symmetry condition is applied on the axis. Additional constraint is imposed separately on the superconducting shield region to force the open shield behavior and formation of the current loops. The total current flowing over the cross-section of the shield (region Ω) must be 0. This constraint is expressed with formula 7.

$$\iint\limits_{\Omega} J_\phi \, dr \, dz = 0 \qquad (7)$$

The model allows to calculate the distribution of magnetic field and find the pattern of shielding currents in the shield. The obtained values are then compared with experimental results and used to predict the changes of the magnetic field homogeneity.

B. Experimental

The assembly of the magnetic shield consists of a tube made of non-magnetic steel and the pieces of superconducting tape attached to its external surface with kapton tape. Their arrangement is similar to the one presented in figure 2a. The tapes are laid on the surface of the tube

and tightly wrapped. The tapes are only partially bent, therefore the shield is not completely circular and the approximation depends on the width of the tape. The layers are shifted with respect to each other by approximately half of the width of the tape. The magnetic shield is placed coaxially inside an electromagnet. The dimensions of the electromagnet and the shield are shown in figure 2b. In the figure the thickness of the shield is neglected. The electromagnet used during the experiments is capable of generating 13.1 mT/A in its center. The electromagnet and the shield are placed in a cryostat and cooled to the temperature of approximately 78 K with liquid nitrogen.

Commercial tape SF12050 by SuperPower Inc. is used as the material for the analyzed shield. Its thickness is 55 μm, with 1 μm of YBCO as a superconducting layer. According to the producer the minimum critical current is 300 A. The width of each tape fragment is 12 mm. Two layers of the tapes are applied. Measurements start with the cool-down of the system at zero-field conditions. After that the current in the magnet is sequentially increased. When a selected value of current is reached the probe is slid along the axis of the magnet using a step motor and the magnetic field is measured. The radial component is measured close to the shield surface, axial - along the axis of the shield and the electromagnet.

The measurements of two components of the field are performed using the probe with two PHE-606817A Hall sensors assembled at Lviv Polytechnic National University. The probes are placed on a probe holder (shown in figure 2c). The holder is attached to a long rod and submerged in liquid nitrogen. The probes are supplied with the current of 10 mA by a current source, as seen in figure 3. The signals from the probes are processed by Keithley Model 2000 digital multimeter and sent to a computer. A second current source is used to supply current to the electromagnet. The electromagnet current is read using the source's internal current meter.

The stepper motor is used to position and move the probe inside the assembly of the electromagnet and the shield. For each step the motor's rotor moves by a constant angle. The probe position is calculated based on the number of steps and the dimensions of the wheel driving the movement of the probe. The readout of the Hall sensor is triggered automatically after each step. The control system was based on an Atmel ATmega microcontroller board connected to the PC. The motor is supplied by DC power supply and controlled by LeadShine M880A step motor driver by the control signals from the microcontroller board, as shown in figure 3. The steering of the motor and data saving are done using the same computer.

C. Homogeneity criterion and empirical formulas

To check the efficiency of the shield in homogenization of the magnetic field a certain criterion has to be devised. In the considered system the ideal situation is the magnetic field with only axial component. B_r should therefore disappear in the shielded region S. To account for these requirements the directional criterion Q_D, connected with B_r, is defined. It is described with formula 8.

$$Q_D = 1 - \frac{\iint\limits_S |B_{rS}| \, dr \, dz}{\iint\limits_S |B_{rNS}| \, dr \, dz} \qquad (8)$$

B_{rS} is the local radial component of the magnetic flux when the shield is applied, B_{rNS} is the analogical value when there is no shield. The criterion can be lower or equal to 1. Ideal field is achieved when its value is 1. It can go below 0, meaning that the application of magnetic shield actually decreases the homogeneity of the field. The criterion describes the level of improvement of the homogeneity of the magnetic field rather than the homogeneity itself. The region S can be defined according to the needs of the particular system. In this paper it is assumed that it corresponds with the region completely surrounded by the shield. In the analysis of experimental results and the comparison with simulations region S denotes the line along which measurement was performed. Then equation 8 becomes one-dimensional. The length of the shielded region for which the criterion is calculated is assumed to be the same as the total length of the electromagnet - 480 mm.

The changes of directional criterion are analyzed for different sizes of the shield and applied currents in the electromagnet. The empirical formula allowing to calculate the directional parameter as the function of diameter, material and number of layers is sought. To generalize the results the considered parameters are reduced according to formulas 9 and 10, for reduced applied electric current J_r and reduced diameter d_r respectively.

$$J_r = \frac{J_e \cdot t_e}{J_{c0} \cdot t_s} \qquad (9)$$

$$d_r = \frac{d_s}{d_m} \qquad (10)$$

J_e is here the average density of electric current in the electromagnet, depending on size of the wire and the number of turns. t_e is the thickness of the electromagnet and t_s is the total thickness of the superconducting layers of the shield. By changing t_s the different number of layers of the shield can be considered. Presence of J_{c0} in formula 9 allows to analyze different materials.

The length of the analyzed shield is the same as of the electromagnet. The aspect ratio between internal diameter of the electromagnet and its length is 1:6. The obtained formula is expected to be valid also for different ratios, since the value of the directional criterion is dominated by changes of the radial component in the region close to the ends of the shield and the electromagnet. To determine the coefficients for the empirical formula
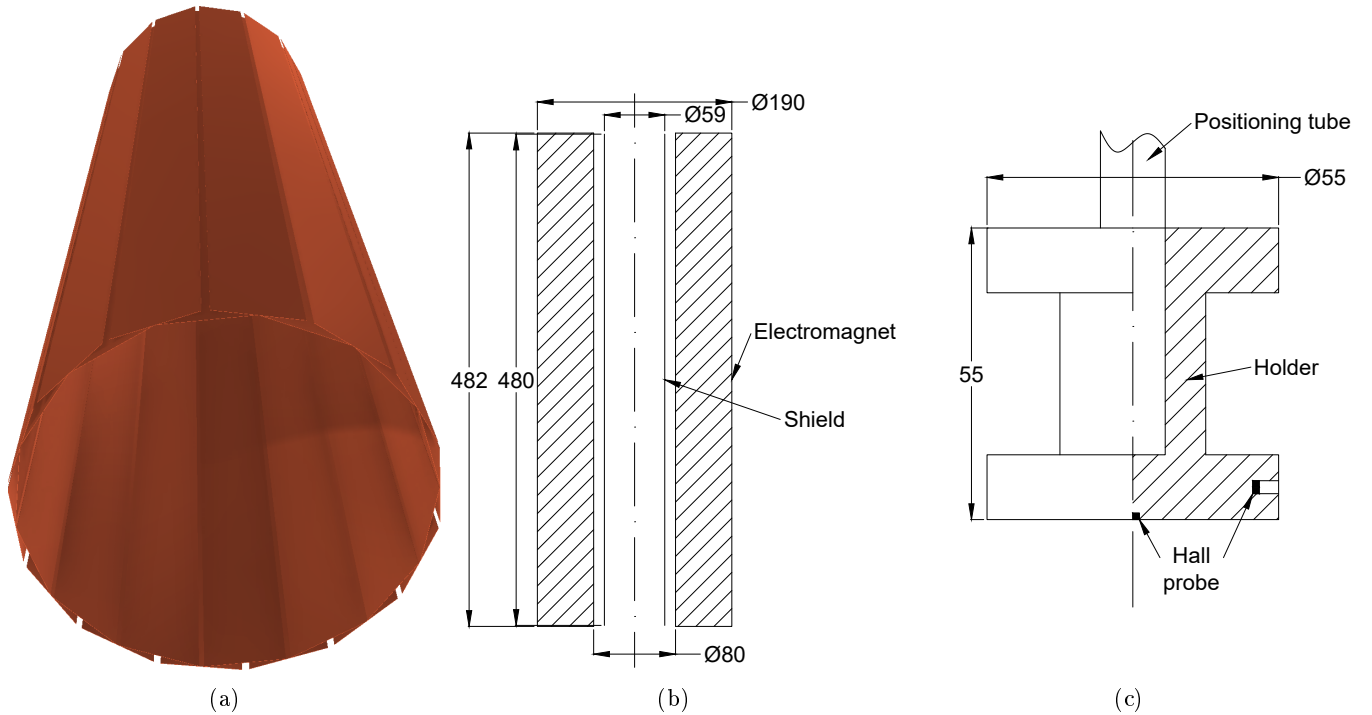
FIG. 2: Elements of the test stand. (a) View of the shield, (b) System dimensions, (c) Probe holder
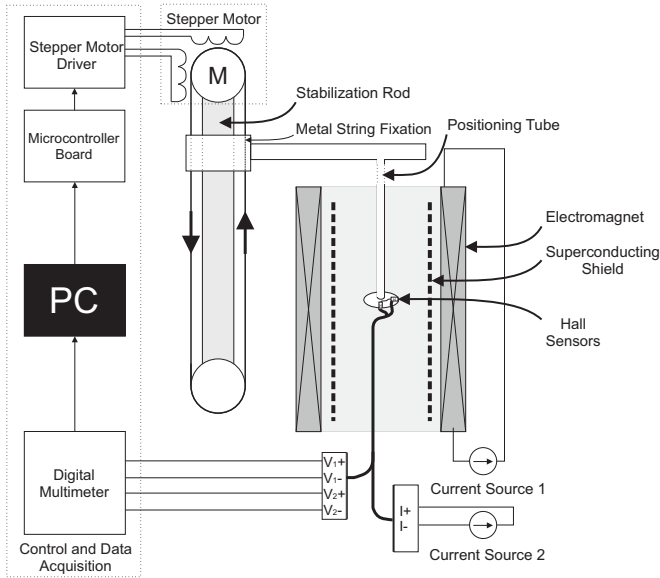

FIG. 3: Scheme of the test stand

III. RESULTS AND DISCUSSION

Comparison between the magnetic flux distribution with and without the magnetic shield found using the numerical model is presented in figure 4. The significant improvement of homogeneity of the magnetic flux in the shielded region is visible. The maximum strength of the magnetic flux is slightly decreased and it is averaged along the shield. The direction of the field is straightened, hinting at the disappearance of B_r.

Improvement of homogeneity is clearly seen when looking at the results of the measurements and calculations shown in figure 5. The value of radial component of the magnetic field measured 1 mm from the internal surface of the shield is presented for the range of electric current applied in the electromagnet up to 10 A. Experimental and model results for the unshielded field are shown for comparison. The value of radial component is normalized to the maximum value calculated with the numerical model for the given applied current at the unshielded configuration. The current applied in the electromagnet is shown to the left, corresponding normalizing value to the right. The results close to center of the assembly are not shown for better visibility of the interesting region. The magnetic field in the central part of the assembly is almost fully homogeneous.

Radial component of the field disappears almost entirely in the shielded region. Close to the end of the shield it quickly increases. Sometimes it is even observed to exceed the maximum value observed in unshielded case, especially in the lower range of an applied magnetic field.

the simulations were performed for four representative values of d_r (0.25, 0.5, 0.75, 0.975) and up to J_r of approximately 10. The resultant formula and coefficients are presented in further section.
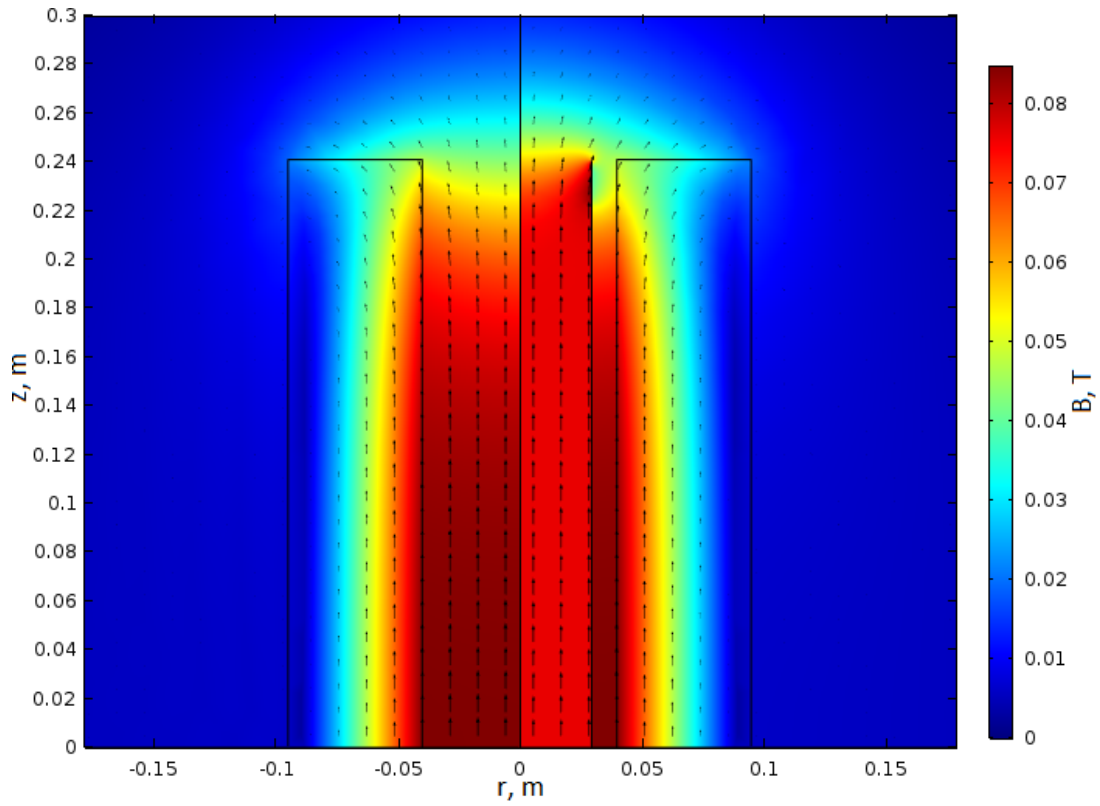
FIG. 4: Comparison between strength and direction of the unshielded (left) and shielded (right) magnetic flux in T with the applied current of 6 A.
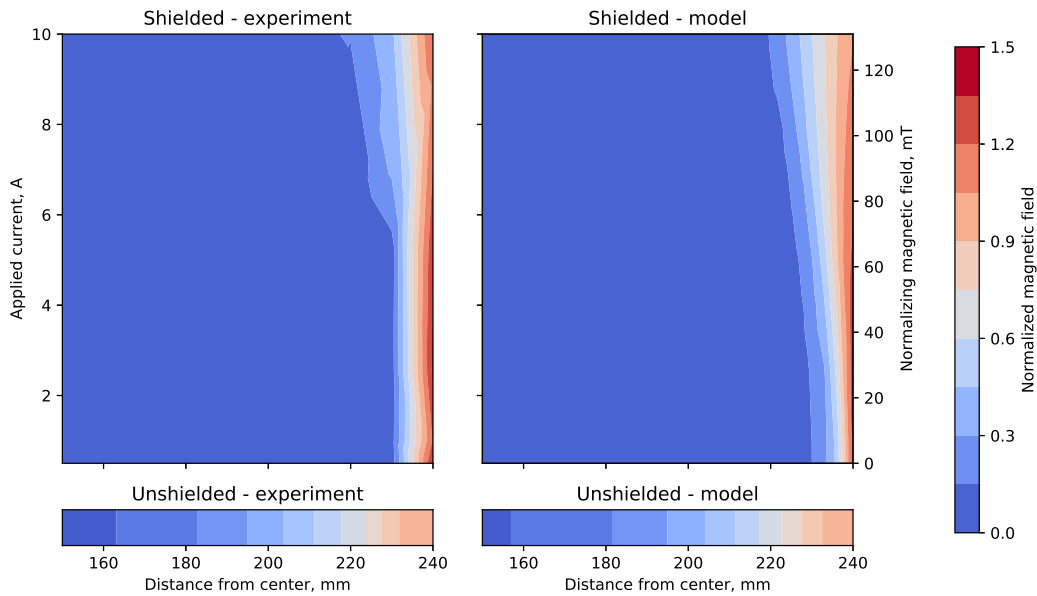

FIG. 5: Normalized radial component of magnetic field in the region close to the end of the shield for different currents in the electromagnet

This effect is due to the concentration of the shielding current at the end of the shield. The total current in this part is significantly higher than in the remaining part of the shield. In the central part of the tape two currents are observed flowing in different direction on each surface. The integration of electric current density over the cross-section of the shield yields zero total current, in accordance with the requirements of the constraint and predictions of the behavior of the open shield.

The size of the region in which the radial component is close to 0 decreases with the strength of the external magnetic field. It happens because the size of the shielding current is limited by the value of the critical current of the superconducting tape. In the considered configuration the angular shielding current is observed to saturate the available current density at the ends of the tape. In the remaining region the current is significantly lower and only partially penetrates the width of the superconducting layer of the tape. When the applied magnetic field is increased, the length of the region in which the current-carrying capacity is filled also grows. Therefore, the distance along which the radial component decreases to 0 becomes larger. Additionally, the critical current of the superconducting tape decreases with the increase of the magnetic field, exacerbating the effect.

Values of directional homogeneity criterion calculated with formula 8 based on the results of modeling and experiments are presented in figure 6a. Consistent with the previously discussed results, the criterion decreases with the increase of the applied magnetic field. According to the model results, if the external field is close to 10 mT the achievable improvement (in the given configuration) is almost 80%. In the field close to 0.13 T it decreases to 65%. Further decrease of shielding quality is expected in higher applied magnetic fields.

The agreement between the experimental and model results is good. Some discrepancy observed in low magnetic fields can be caused by the slight misplacement of the measuring probe. The assumption that the effects of the shielding currents flowing in z direction in the neighboring tapes cancel each other seems to be correct. No additional shielding effect or disturbances coming from these currents are observed experimentally. The numerical model is able to properly predict shielding efficiency of the shield if proper material data are available, even despite the simplifications. Thanks to the application of 2D axial geometry, the proposed approach allows to significantly decrease computation time and eases the analysis of the results. The approximate time of calculation of a single magnetic field distribution is 30 minutes, with slightly less than 30000 nodes. The time of computations depend on the applied magnetic field and the degree of saturation of the shield region with current.

The results of analysis of the shield operation in wide range of diameters and applied currents are shown in figure 6b. Empirical formulas are formed to allow prediction of the value of Q_D for different combination of J_r and d_r.
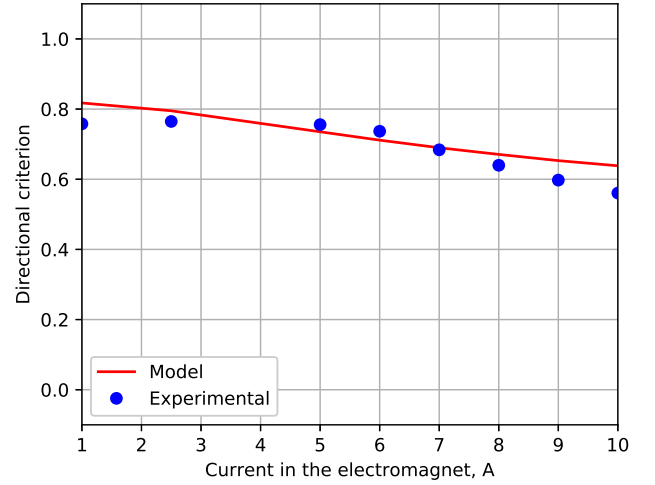
(a)
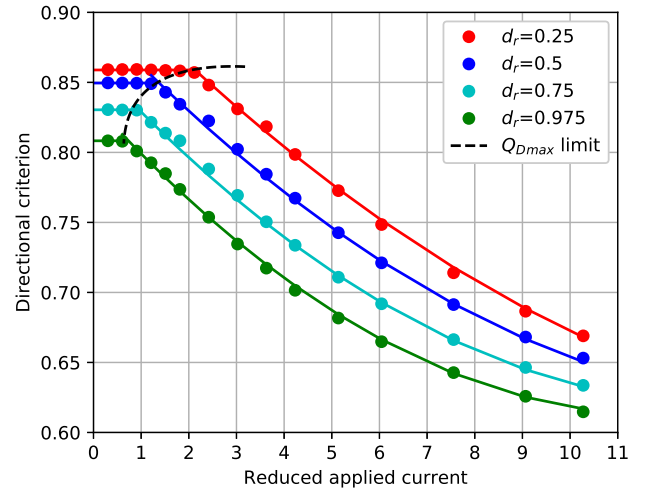
(b)

FIG. 6: Directional criterion of shielding quality. (a) Comparison of experimental and numerical results, (b) Calculated and simulated effect of shield size and strength of applied magnetic field

Up until a certain threshold value of J_{rt} depending on d_r the value of Q_D remains constant for a given d_r. To calculate this value, marked as Q_{Dmax}, for a given d_r, fomula 11 can be used.

$$Q_{Dmax}(d_r) = 0.86 + 0.007 \cdot d_r - 0.063 \cdot d_r^2 \qquad (11)$$

J_{rt} is calcuted with formula 12.

$$J_{rt}(d_r) = 3.18 - 4.99 \cdot d_r + 2.44 \cdot d_r^2 \qquad (12)$$

In the region with constant Q_D the superconducting layer has sufficient current-carrying capacity to nullify a radial component of magnetic field possible to be affected with given geometry. It can be seen that if the shield has the

same length as the solenoid it is not possible to entirely remove the radial component. Decrease of J_{rt} with r_d is connected with changes of shape of a solenoidal magnetic field with the relative distance from an axis. On the axis the field is entirely straight, farther from it the total radial component encountered by the shield increases.

Above J_{rt} the superconducting current in the shield is insufficient to maintain its constant attenuating ability and Q_D starts to decrease. Changes of d_r affect value of Q_D similarly to previous case, by changing the total value of radial component in the shielded region. Q_D in the entire considered region can be calculated with formula 13.

$$Q_D = \begin{cases} Q_{D\,max} & \text{when } J_r < J_{rt} \\ a + b \cdot J_r + c \cdot J_r^2 & \text{when } J_r \geq J_{rt} \end{cases} \quad (13)$$

a, b and c are found with formula 14, 15 and 16, respectively.

$$a = 0.96 - 0.13 \cdot d_r \quad (14)$$

$$b = -0.034 - 0.0032 \cdot d_r \quad (15)$$

$$c = 0.00072 + 0.000875 \cdot d_r \quad (16)$$

The presented results suggest some ways to improve the efficiency of the shields in homogenization of the magnetic field. The most important is the increase of current carrying capacity. Decrease of r_d also leads to increase of homogenizing abilities of the shield, but limits its usefulness by decreasing the size of the shielding region.

The increase of the current carrying capacity can be achieved by adding more layers of the superconducting tape to the shield or by slight changes of geometry. Spiral arrangement of the tapes could promote the flow of the shielding currents in the direction in which the anisotropic tapes exhibit the highest critical current density. Such pattern is complex to manufacture and can increase the production costs. Another way is to decrease the operating temperature of the shield. This approach rises spending on cooling. Finally, different type of tapes with higher current density can be used. However, it would can the availability of the material and increase its price.

The proposed solution is advantageous as it allows to utilize short pieces of tapes, which normally are considered a by-product in the production of longer pieces. The length of the piece of tape required to produce the shield corresponds with the dimensions of a shielded region. Interaction chamber of the electron cooling system for NICA will have length of 2 m, typical length of scanner bore in MRI is close to 1 m. Comparing this values with typical length of short pieces of tapes offered by the producers it can be seen that the material to produce the open superconducting magnetic shields is readily available and abundant. This and the simple construction of the proposed shields predestines them to be applied in multiple systems for the control of the shape of magnetic field.

IV. CONCLUSIONS

Significant improvement of homogeneity over a long shielded is successfully obtained with the application of the open magnetic shield. The radial component of the magnetic field is decreased over almost entire length of the shielded region. The improvement of homogeneity decreases with the increase of the external magnetic field due to the limitation set by critical current density of the tape. The results of numerical modeling agree well with the experimental ones. The proposed screens are cheap and efficient method of improving the homogeneity of magnetic field even in large regions. Analysis of the results suggests the methods to further improve the efficiency of the shields. It can be done using the tapes with higher critical current and by the increase of the number of layers of the shield.

The proposed superconducting shields can find application in the devices requiring homogeneous magnetic fields as the method of obtaining the desired magnetic field shape, such as electron cooling system and MRI devices. They can also increase the length of homogenous region in magnets, for example ones used for the characterization of superconducting cables. The design of the shield for specific application is fast using the proposed simplified numerical model. Further research on the open magnetic shields is planned, including the application of new materials and geometries and analysis of behavior in other configurations of an applied magnetic field.

REFERENCES

[1] Z. Bunzarov, V. Dodokhov, A. Efremov, V. Golovatyuk, V. Ionaites, V. Kekelidze, O. Kovalchuk, E. Koshurnikov, Y. Lobanov, A. Makarov, V. Ochrimenko, and A. Vodopyanov, International Conference on Instrumentation for Colliding Beam Physics, Budker Institute of Nuclear Physics, Novosibirsk, Russia (2014).

[2] N. Agapov, D. Donets, V. Drobin, E. Kulikov, H. Malinowski, R. Pivin, A. Smirnov, Y. Prokofichev, G. Trubnikov, and G. Dorofeev, Proceedings of COOL'11, Alushta, Ukraine , 118 (2011).

[3] I. Frollo, P. Andris, A. Krafčík, D. Gogola, and T. Dermek, IEEE Transactions on Magnetics **54**, 1 (2018).

[4] T. Wang, S. Xiao, X. Liu, and Y. Li, IEEE Transactions on Applied Superconductivity **26**, 4301904 (2016).

[5] D. Qiu, W. Wu, Y. Pan, Z. Y. Li, Y. Wang, S. Chen, Y. Zhao, Z. Zhang, P. Yang, X. B. Meng, J. Z. Tian, Y. Q. Zhou, Z. Hong, and Z. Jin, IEEE Transactions on Applied Superconductivity **27**, 4601505 (2017).

[6] W. Williams, M. Stephen, and C. Lane, Physics Letters **9**, 102 (1964).

[7] A. Hinterberger, S. Gerber, and M. Doser, Journal of Instrumentation **12**, T09002 (2017).

[8] Ł. Tomków, M. Ciszek, and M. Chorowski, Journal of Applied Physics **117**, 043901 (2015).

[9] K. Hogan, J.-F. Fagnard, L. Wéra, B. Vanderheyden, and P. Vanderbemden, Supercond. Sci. Technol. **31**, 015001 (2018).

[10] L. Wéra, J. Fagnard, D. K. Namburi, Y. Shi, B. Vanderheyden, and P. Vanderbemden, IEEE Transactions on Applied Superconductivity **27**, 6800305 (2017).

[11] L. Wéra, J. Fagnard, K. Hogan, B. Vanderheyden, D. K. Namburi, Y. Shi, D. A. Cardwell, and P. Vanderbemden, IEEE Transactions on Applied Superconductivity **29**, 6801109 (2019).

[12] L. Prigozhin and V. Sokolovsky, Journal of Applied Physics **123**, 233901 (2018).

[13] D. Qiu, J. Zhang, B. Wei, H. Huang, F. Gu, Z. Li, Z. Huang, W. Wu, D. Hu, J. Jiang, Z. Hong, and Z. Jin, IEEE Transactions on Applied Superconductivity **27**, 1 (2017).

[14] J. Kvitkovic, S. Pamidi, and J. Voccio, Supercond. Sci. Technol. **22(12)**, 3577 (2009).

[15] Y. Nagasaki, M. Solovyov, and F. Gömöry, IEEE Transactions on Applied Superconductivity **28**, 6601905 (2018).

[16] Ł. Tomków, M. Ciszek, and M. Chorowski, IEEE Transactions on Applied Superconductivity **26**, 1 (2016).

[17] J. Kvitkovic, D. Davis, M. Zhang, and S. Pamidi, IEEE Transactions on Applied Superconductivity **23(3)**, 8200605 (2013).

[18] L. Wéra, J. Fagnard, G. Levin, B. Vanderheyden, and P. Vanderbemden, IEEE Transactions on Applied Superconductivity **23(3)**, 8200504 (2013).

[19] L. Wéra, J. Fagnard, G. Levin, B. Vanderheyden, and P. Vanderbemden, Supercond. Sci. Technol. **28**, 074001 (2015).

[20] J. Kvitkovic, S. Patel, M. Zhang, Z. Zhang, J. Peetz, A. Marney, and S. Pamidi, IEEE Transactions on Applied Superconductivity **28**, 1 (2018).

[21] R. S. Bakolo, R. van Staden, P. Febvre, and C. J. Fourie, Journal of Superconductivity and Novel Magnetism **30**, 1649 (2017).

[22] H. Qian, P. Zhou, and G. Ma, IEEE Magnetics Letters **8**, 1309104 (2017).

[23] F. Gömöry, M. Solovyov, J. Šouc, C. Navau, J. Prat-Camps, and A. Sanchez, Science **335**, 1466 (2012).

[24] K. Capobianco-Hogan, R. Cervantes, A. Deshpande, N. Feege, T. Krahulik, J. LaBounty, R. Sekelsky, A. Adhyatman, G. Arrowsmith-Kron, B. Coe, K. Dehmelt, T. Hemmick, S. Jeffas, T. LaByer, S. Mahmud, A. Oliveira, A. Quadri, K. Sharma, and A. Tishelman-Charny, Nuclear Instruments and Methods in Physics Research Section A: Accelerators, Spectrometers, Detectors and Associated Equipment **877**, 149 (2018).

[25] M. Solovyov, J. Šouc, F. Gömöry, M. O. Rikel, E. Mikulášová, M. Ušáková, and E. Ušák, IEEE Transactions on Applied Superconductivity **27**, 1 (2017).

[26] W. Xu, X. Liu, S. Du, and J. Zheng, Fusion Engineering and Design **118**, 20 (2017).

[27] J. Geng, H. Zhang, C. Li, X. Zhang, B. Shen, and T. Coombs, Supercond. Sci. Technol. **30**, 035022 (2017).

[28] M. Masuzawa, A. Terashima, K. Tsuchiya, and R. Ueki, Supercond. Sci. Technol. **30**, 034009 (2017).

[29] A. Smirnov, G. Dorofeev, V. Drobin, E. Kulikov, and H. Malinovski, Physics of Particles and Nuclei Letters **13**, 949 (2016).

[30] S. Slutsky, C. Swank, A. Biswas, R. Carr, J. Escribano, B. Filippone, W. Griffith, M. Mendenhall, N. Nouri, C. Osthelder, A. P. Galván, R. Picker, and B. Plaster, Nuclear Instruments and Methods in Physics Research Section A: Accelerators, Spectrometers, Detectors and Associated Equipment **862**, 36 (2017).

[31] E. Kulikov, N. Agapov, V. Drobin, A. Smirnov, G. Trubnikov, G. Dorofeev, and H. Malinowski, Journal of Physics: Conference Series **507**, 032028 (2014).

[32] R. Pecher, M. McCulloch, S. Chapman, and L. Prigozhin, Proc. EUCAS 2003 (2003).

[33] M. Zhang, J. Kvitkovic, J.-H. Kim, C. H. Kim, S. V. Pamidi, and T. A. Coombs, Applied Physics Letters **101**, 102602 (2012).

[34] M. Zhang, J.-H. Kim, S. Pamidi, M. Chudy, W. Yuan, and T. A. Coombs, Journal of Applied Physics **111**, 083902 (2012).

[35] X. Zhang, Z. Zhong, J. Geng, B. Shen, J. Ma, C. Li, H. Zhang, Q. Dong, and T. A. Coombs, Journal of Superconductivity and Novel Magnetism (2018), 10.1007/s10948-018-4678-8.